Generation of the Amundsen Sea Low by Antarctic orography

Rishav Goyal[1,2,*], Martin Jucker[1,2], Alex Sen Gupta[1,2,3] and Matthew H England[1,2,3]

1. Climate Change Research Centre, University of New South Wales, NSW, 2052 Australia

2. ARC Centre of Excellence for Climate Extremes, University of New South Wales, NSW, Australia

3. Australian Centre for Excellence in Antarctic Science (ACEAS), University of New South Wales, NSW, Australia

---

[*]*Corresponding author: rishav.goyal@unsw.edu.au*

Key points

1. The Amundsen Sea Low owes its existence to an interaction between the westerly wind jet and Antarctic orography

2. Mountains in the West Antarctic region trap the low-pressure system in the Amundsen-Bellingshausen Seas region

3. Teleconnections from low latitudes have little to no role in generating the climatological Amundsen Sea Low

Abstract

The Amundsen Sea Low (ASL) is a distinctive feature of the Southern Hemisphere (SH) high latitude atmospheric circulation, regulating regional Antarctic climate, meridional heat transport, ocean circulation, and sea-ice in the Amundsen-Bellingshausen Seas. Most previous research on the ASL has focused on its variability with only a few studies attempting to understand why the climatological ASL exists. These studies have proposed different hypotheses to explain the presence of ASL, however, a clear understanding of the mechanisms responsible for the generation of the ASL remains uncertain. Here we use an atmospheric general circulation model to show that the ASL is a consequence of the interaction between Antarctic topography and the westerly wind jet, with negligible influence from low-latitude teleconnections. A non-rotating fluid flow simulation further suggests that the ASL can be explained by flow separation resulting from the interaction of westerly winds with the topography of Antarctica.

Plain Language Summary

The Amundsen Sea Low is the climatological low-pressure center present in the south Pacific sector of the Southern Ocean. This low-pressure center significantly affects temperature, precipitation, sea-ice and ice shelves in the West Antarctica region. Various hypotheses have been suggested to explain the mechanisms responsible for the existence of the ASL. However, a clear understanding of the generation mechanisms is not yet available. In this study, we use a state-of-the-art climate model to test the previously suggested mechanisms and show that the ASL is generated by an interaction between the westerly winds with Antarctic orography, with negligible influence from low latitudes.

Introduction

The Amundsen Sea Low (ASL) is a persistent climatological low-pressure center located in the South Pacific sector of the Southern Ocean between the Antarctic Peninsula and the Ross Sea (Hosking et al., 2013). The ASL is the deepest climatological low-pressure center globally and is located in the circumpolar trough around Antarctica between 60-75°S (Raphael et al., 2016; Turner et al., 2013). It is a key component of the non-zonal climatological circulation in the southern high latitudes and is commonly called the "pole of variability" (Lachlan-Cope et al., 2001) as it exhibits strong intra-seasonal to interannual variability in the Southern Hemisphere extratropical circulation. The ASL significantly impacts West Antarctic climate, including temperature, sea-ice extent and precipitation via variability in the meridional wind field and ocean circulation (see e.g. Hosking et al., 2013; Raphael et al., 2016; Turner et al., 2016).

The ASL has undergone a significant deepening trend in recent decades but only during austral summer (England et al., 2016). This summertime deepening trend has been attributed to the positive trend in the Southern Annular Mode (SAM, England et al., 2016; Raphael et al., 2016; Hosking et al., 2016), driven primarily by stratospheric ozone depletion, with greenhouses gases playing a secondary role (Arblaster & Meehl, 2006; Thompson et al., 2011). Deepening of the ASL has been suggested to have modified ocean circulation and heat transport onto the Antarctic shelf, leading to rapid ice loss from west Antarctic glaciers (Pritchard et al., 2009; Thoma et al., 2008). The ASL is projected to deepen further in the future because of the expected ongoing positive trend in the SAM (Hosking et al., 2016; Raphael et al., 2016). The projected positive trend in the SAM manifests as higher MSLP in the Southern Hemisphere (SH) extratropics and lower MSLP in the SH polar latitudes (Hosking

et al., 2016; Raphael et al., 2016). Future changes in the SAM (and therefore ASL) are projected to be dominated by an increase in greenhouse gases (Raphael et al., 2016), with recovering ozone playing a lesser role (Goyal et al., 2020a; Thompson et al., 2011).

Given the importance of the ASL for changes in the West Antarctic region, including its impacts on the West Antarctic Ice Sheet, most previous work has focused on the variability of the ASL pattern and on its past and projected changes as well as their implications for the West Antarctic climate. However, only a small number of studies have focused on what gives rise to the climatological ASL in the first place. In particular, Baines & Fraedrich (1989) were the first to consider this problem, conducting rotating tank experiments with a physical scaled-down model of Antarctica, including realistic orographic features placed in homogeneous (fresh water) and stably stratified fluid. Their results suggested that the ASL might be generated by flow separation because of an interaction between the westerly jet in the southern high latitudes and Antarctic orography (refer to Fig. 1a showing Antarctic orography). However, quantitative assessment was not possible with their experimental set-up, with the model results based on visual inspection of the flow. Subsequently, Walsh et al., (2000), using a simple 2-layer baroclinic model of the atmosphere, found a weak ASL pattern in simulations with a flat Antarctic land-mass (i.e. no orography over Antarctica). They suggested that even though the baroclinicity created because of the presence of Antarctic orography strengthens the ASL pattern, the climatological low pressure might be generated either by the shape of the Antarctic continent or because of synoptic activity from the SH mid-latitudes in the absence of Antarctic topography. Both these studies were carried out using a simplified representation of the Antarctic climate system, omitting important physics such as katabatic winds, and with limited representation of Antarctic orography and stationary waves

in the atmosphere. More recently, Fogt et al., (2012) used multiple reanalysis products to suggest that the ASL might be generated and maintained by a net influx of cyclonic storms reaching the ASL region. They proposed that the ASL is present in the climatological mean because of the high density of cyclonic storms from both lower latitudes and from the baroclinic zone around Antarctica ending up in the Amundsen-Bellingshausen Seas. However, Raphael et al. (2016) found that the seasonal location of the ASL does not always coincide with the center of maximum storm activity. Several other recent studies (e.g., Yiu & Maycock, 2019; Yiu & Maycock, 2020) have linked the existence of the ASL to zonal asymmetries in tropical sea surface temperatures (SSTs) via planetary scale Rossby wave activity from the tropics to the southern high latitudes.

Given these competing hypotheses, a clear understanding of the mechanisms responsible for the generation of the ASL remains uncertain. In this study, we use an atmospheric general circulation model supplemented with a non-rotating fluid dynamics simulation, to examine the mechanisms responsible for the generation of the Amundsen Sea Low.

Climate model

We use the National Centre for Atmospheric Research (NCAR) Community Earth System Model (CESM v1.2.2) which was part of the Coupled Model Intercomparison Project 5 (CMIP5). The atmospheric component of the model is the Community Atmosphere Model Version 4 (CAM4, Neale et al., 2010) and is coupled to the Community Land Model Version 4 (CLM4, Oleson et al., 2010). CAM4 is run with a 1.875 x 2.5° finite volume grid with 26 hybrid sigma levels. CAM4 is forced with monthly averaged interannually varying SSTs and sea-ice.

SST and sea-ice fields are obtained from a fully coupled run of NCAR CESM integrated in a pre-industrial control configuration.

A Computational Fluid Dynamics (CFD) analysis in a non-rotating frame of reference is also carried out using the *ANSYS Fluent Academic Research* v2019 R3 fluid dynamics simulation software. A smoothed 3-dimensional model of Antarctica on a Mercator projection is constructed using the *ANSYS SpaceClaim* software over a coarse tetrahedron mesh for numerical discretization. The height of Antarctica is kept constant at all longitudes. This idealized 3-D model of Antarctica is placed in a westerly wind flow of 10 m/s, matching the typical climatological westerly wind velocity around Antarctica. In the real world, easterlies driven by the effects of gravity (katabatic winds) and the pressure gradient force are present near the edge of the Antarctic orography. These polar easterlies are not present in this simulation, but the model configuration is reasonable because the effect of these katabatic winds on the localised circulation features around Antarctica is minimal compared to the westerlies (Baines and Fraedrich, 1989). Moreover, in the region west of the Ross Sea and near the Antarctic Peninsula, these easterlies are only present for a few hundred meters above the surface, with the climatological winds aloft being the prevailing westerlies.

Model Simulations

Model simulations with NCAR CESM were carried out to understand the generation of the ASL pattern. For all simulations, the model uses a pre-industrial control configuration (i.e. pre-industrial levels of greenhouse gases, aerosols and other forcing). A control simulation (*CTRL*, Fig. 1b) is carried out with interannual varying monthly SSTs and sea-ice. The control

simulation has a realistic land-sea configuration as well as realistic orography over all landmasses including Antarctica. A second simulation (NO_{TOPO}, Fig. 1c) is carried out in which the topography is removed everywhere (i.e. flat land at sea level). Another simulation (ANT_{TOPO}, Fig.1d) is then integrated in which only the topography over Antarctica is added to the NO_{TOPO} simulation. In a third experiment (*EAST-*ANT_{TOPO}, Fig.1e), topography is only present over East Antarctica (i.e. topography over the West Antarctic including the Antarctic Peninsula is flattened to sea level). Finally, in the $ROTATED_{ANT}$ (Fig.1f) simulation, Antarctica is rotated by 100 degrees towards the west, while all other land-ocean features north of Antarctica remain at the same location as in the *CTRL* simulation. SST and sea-ice fields south of 62°S are also rotated by 100 degrees west in the $ROTATED_{ANT}$ simulation. To remove any sudden discontinuities in SST and sea-ice fields in the $ROTATED_{ANT}$ simulation, both SST and sea-ice fields are smoothed using linear interpolation in the buffer region between 57-62°S. All simulations are integrated for 120 years. The first 20 years are discarded as a spin-up period and the remaining 100 years are used for the analyses presented here.

Data and methods

Monthly mean sea level pressure (MSLP) and surface (at 60-m elevation) zonal winds from the model simulations are analysed in this study. Monthly averaged MSLP from the European Centre for Medium Range Weather Forecasts (ECMWF) Reanalysis (ERA-Interim; Dee et al., 2011) from 1979-2016 is also used for model evaluation. The ASL index is defined as the minimum MSLP in the South Pacific sector of the Southern Ocean (between 60-75°S and 180-310°E; after Turner et al., 2013). For the $ROTATED_{ANT}$ simulation, ASL is calculated as minimum MSLP between 60-75°S and 80-210°E. As the zonal mean MSLP in simulations with differing topography and / or land-sea configurations is found to be different, a relative ASL index is

used. The relative ASL index is defined as the minimum MSLP between 60-75°S and 180-310°E after the zonal mean MSLP has been removed.

Climatological mean ASL

For the purposes of model validation, the simulated ASL from *CTRL* is compared with the ERA-Interim reanalysis (Fig. 2a, b). The model is able to capture the magnitude, location and spatial extent of the ASL with reasonable fidelity. The simulated climatological mean ASL is at approximately the same location as the ERA-Interim reanalysis, however, the simulated ASL in *CTRL* is deeper when compared to ERA-Interim (Fig. 2). The simulated zonal mean MSLP around Antarctica in *CTRL* is also lower compared to the reanalysis. In fact, after removing the zonal mean, the relative ASL is actually deeper in the ERA-Interim reanalysis as compared to *CTRL* (Fig. 2c, d).

To examine the role of orography in generating the ASL pattern, the NO_{TOPO} simulation (Fig. 1c) is carried out in which all landmasses are set to a fixed flat sea level elevation in the model (i.e. the topography is removed everywhere). In this simulation, no climatological low-pressure centre is found in the Amundsen Sea region (Fig. 1c), suggesting a critical role played by topography in generating the ASL pattern. The zonal wave 1 pattern present in the SH mid-latitudes found in the *CTRL* simulation (Fig. 1b) shifts poleward in the NO_{TOPO} simulation because of the absence of any topographic barrier provided by Antarctica, and therefore a clear zonal wave 1 pattern is now present around Antarctica with a high pressure in the Amundsen Sea region (Fig. 1c). This result contrasts the findings of Walsh et al., (2000) who found an ASL to be present, albeit much weaker, in the absence of Antarctic orography using a simple 2-layer baroclinic model.

Next, we examine the role played by orography over Antarctica alone in generating the ASL pattern. To do this, another simulation (ANT_{TOPO}) is integrated in which only topography over Antarctica is added to the NO_{TOPO} simulation (Fig. 1d). In this experiment a clear low-pressure centre is now present in the Amundsen Sea region (Fig. 1d) with an ASL magnitude almost as deep as in *CTRL* (10.8 hPa in ANT_{TOPO} compared to 11.2 hPa in CTRL). The location of the ASL is also similar to *CTRL* (76.7°S, 201°E in ANT_{TOPO} and 76.7°S, 202°E in *CTRL*). The climatological pressure field around Antarctica is marginally weaker in the ANT_{TOPO} simulation as compared to *CTRL*, however the strength and location of the ASL relative to the ambient large-scale pressure field are comparable (e.g. compare Figs. 1b and 1d). Clearly the presence of Antarctic topography can largely explain the presence of the ASL pattern.

Next, to examine the factors controlling the climatological location of the ASL, another simulation (*EAST-*ANT_{TOPO}) is integrated in which topography over western Antarctica (including over the West Antarctic Ice Sheet and the Antarctic Peninsula) is removed (Fig. 1e), while East Antarctic topography remained unchanged. The climatological location of the ASL in this simulation shifts eastward towards the Antarctic Peninsula and the ASL is no longer trapped in the Amundsen-Bellingshausen Seas region as found in *CTRL* (Fig. 1e). This clearly shows that the mountains in the western part of Antarctica constrain the low-pressure centre in the Amundsen Sea region.

Zonal variability in the tropical heating can create stationary waves in the SH high latitudes (Trenberth et al., 1998; Inatsu and Hoskins 2004; Goyal et al., 2020b). Several past studies have demonstrated a strong influence of the tropics in generating ASL variability (Clem et al., 2017; Pope et al., 2017; Raphael et al., 2016). Zonal variability in tropical heating has strong

impacts on the ASL via upper tropospheric planetary Rossby waves which move poleward and eastward from their tropical source region (Inatsu & Hoskins, 2004). These waves are present in the climatological mean and also show strong variability at monthly to interannual timescales. The climatological mean ASL is located southward of the crest of the climatological Zonal Wave 1 in the SH extratropics, which is known to be strongly influenced by deep convection over the Indo-Pacific warm pool in the tropics (Peña-Ortiz et al., 2019). As such, zonal asymmetries related to tropical heating may be expected to play a role in setting the characteristics of the climatological mean ASL, as it does for example for the Zonal Wave 3 pattern (Goyal et al., 2020b). To test this possibility, another simulation ($ROTATED_{ANT}$) is carried out in which Antarctica is rotated westward by 100 degrees while all other landmasses are kept at the same location as in *CTRL* (refer to Fig. 1f and methods for details). Even though the Amundsen-Bellingshausen Seas are now away from the climatological zonal wave 1 crest, a clear ASL pattern is still found in this simulation (Fig. 1f). Furthermore, there is no change in the depth of the ASL in the $ROTATED_{ANT}$ simulation compared to *CTRL* (11.2 hPa in both $ROTATED_{ANT}$ and *CTRL*). There is also almost no change in the zonal location relative to the Antarctic continent; i.e., it is now shifted westward by 100 degrees similar to the 100 degrees westward shift of the Antarctic landmass in this simulation (101.5°E in $ROTATED_{ANT}$ and 202°E in *CTRL*). Even though there is a northward shift in the meridional location of the ASL in the $ROTATED_{ANT}$ simulation as compared to CTRL, its magnitude is rather small (74.9°S in $ROTATED_{ANT}$ and 76.7°S in *CTRL*). These results suggest that tropical teleconnections have little role in the characteristics of the climatological mean ASL.

Mechanism

We next examine whether the climatological ASL is a consequence of the large-scale surface

westerlies, for example, as a result of flow separation due to orographic features over Antarctica. To help understand this, we examine how variability in the strength of the large-scale mid-latitude westerly winds affects the ASL. Care must be taken while interpreting these results, as these variables are not independent of each other. Moreover, the relationship might also be influenced by the large-scale variability related to the SAM, which manifests as a seesaw in the pressure field between SH mid-latitudes and Antarctica. In this analysis we find that there is a large-scale relationship between the strength of the surface westerlies and the ASL beyond the local effect of the ASL (Fig. 3a). In particular, a significant correlation of -0.59 is found between the strength of the large-scale mid-latitude westerly wind anomalies and the ASL index anomaly, with a deeper ASL associated with stronger surface westerlies (Fig. 3a) suggesting a persistent relationship between the interannual variability in the mid-latitude westerly winds and the ASL. Moreover, the seasonal variability in the depth of the ASL is also strongly related to the seasonal variability in the strength of the mid-latitude westerlies (Fig. 3b). In particular, the depth of the climatological ASL shows a maximum during austral spring consistent with the stronger mid-latitude surface westerlies during this season, and it exhibits a minimum during austral fall consistent with weaker westerly winds during fall (Fig. 3b).

The previous analysis suggests that stronger westerlies may generate a stronger ASL. Following on from the previous analysis, we next test whether the ASL-like clockwise circulation can be created by flow separation due to the interaction of westerly winds with the topography over Antarctica. To do this, we undertake an idealised experiment in a non-rotating frame of reference where a westerly wind (with realistic strength) is introduced at the western boundary, to the west of the Ross Sea, and allowed to interact with the Antarctic

coastline. The 3-D model of Antarctica has a smoothed yet realistic shape of the Antarctic continent. In this model there is no variation in wind strength or topography with height (i.e. equivalent to a 2-D barotropic model). The model configuration is reasonable given that the circulation at polar latitudes is equivalent barotropic (Turner et al., 2013). The model is placed in an idealized westerly flow of 10 m/sec (equivalent to the climatological zonal mean surface westerly wind strength near the Antarctic margin) and 50 ensembles are carried out with each ensemble comprising of 200 simulation time-steps. The simulation clearly shows that a clockwise circulation is generated in the lee of Victoria Land due to the interaction between the westerly winds and Antarctic topography (Fig. 4). The westerly flow adjacent to the continent separates from the coast as it reaches the Ross Sea embayment. This gives rise to a cyclonic circulation that extends to the Antarctic Peninsula. This flow separation can be understood as similar to a flow around a solid body; for example, a sphere or an aircraft wing, which forms lee side eddies because of separation of the flow from the surface. The clockwise circulation is contained in the Amundsen-Bellingshausen Seas region by the topography in the West Antarctic region including the Antarctic Peninsula.

Conclusions

Multiple hypotheses have been suggested in the past to explain the generation of the climatological mean ASL in the southern high latitudes. In this study, we put these hypotheses to the test and then further examined the mechanisms responsible for creating the climatological ASL using an atmospheric general circulation model as well as a non-rotating fluid dynamics simulator. We show that the ASL is generated because of the presence of Antarctic topography interacting with the westerly wind jet, and that it is trapped in the Amundsen-Bellingshausen Seas because of the presence of topography in the west Antarctic

region. We also show that teleconnections from the tropics have little to no role in generating the climatological ASL pattern. A simulation carried out using a fluid dynamics simulator further suggests that an ASL-like clockwise circulation can be generated by flow separation using an idealized Antarctic landmass in the presence of westerly airflow, without the effects of rotation.

Our results show that the ASL is a consequence of the interaction between westerly airflow with the topography of Antarctica, however, easterlies are present close to the Antarctic margin, which are generated from downslope katabatic winds. These katabatic winds may also have a role in controlling the depth and location of the climatological mean ASL. The katabatic winds are stronger in the Ross Sea sector of Antarctica (Parish and Cassano, 2003) and even though they may play a role in modulating the climatological mean ASL, it is difficult to disentangle the effects of katabatic winds from the effects of flow separation by Antarctic topography in a climate model. An attempt to do this was made by Parish & Cassano (2003), who tried to disentangle the effects of katabatic winds from the effects of Antarctic topography by running climate model simulations without explicit longwave radiation. Although they were able to suppress katabatic winds in their model simulations, they however found that the low-level winds resulting from the pressure gradient force resembled katabatic winds, with directions being tied to the underlying terrain. Even with this limitation of not being able to disentangle these two effects, our results still strongly suggest that the ASL is a consequence of the Antarctic topography alone, as the katabatic winds themselves are present only because of the existence of elevated Antarctic topography. Despite the generation of the ASL being related to regional westerly flow – topography interactions, the variability of the ASL is influenced by remote factors. For example, tropical variability related

to the El-Niño Southern Oscillation (ENSO) can create significant changes in the depth of the ASL during the austral winter, with depth of the ASL being significantly lower during the La-Niña phase of ENSO as compared to the El-Niño phase (Turner et al., 2013; Raphael et al., 2016). The Southern Annular Mode (SAM) which manifests as a seesaw in atmospheric pressure between Southern mid- and high-latitudes is also known to control variability in the ASL (Turner et al., 2013) with the ASL being deeper during the positive phase of the SAM and shallower during the negative phase. These variations are effectively superimposed on the climatological mean ASL pattern, which we have shown here to be due to an interaction between the westerly wind jet and Antarctic orography.

Data availability statements

All data analyzed in this study are freely available to download. ERA-Interim data can be downloaded from the ECMWF website (https://www.ecmwf.int/en/forecasts/datasets/reanalysis-datasets/era-interim). Data for the atmospheric model simulations required to reproduce the figures is available at https://data.mendeley.com/datasets/ftx4jskww7/draft?a=971a3bcd-5050-4b9d-b505-febb4d8f5cfd.

Acknowledgements

This study was supported by the Australian Research Council (grants CE170100023, FL150100035). We would like to thank Dr. Andrea Taschetto from the Climate Change Research Centre for generously providing the monthly varying SSTs and sea-ice data used to force the atmospheric model simulations. R.G. is supported by the Scientia PhD scholarship from the University of New South Wales. M.H.E. is also supported by the Earth Science and

Climate Change Hub of the Australian Government's National Environmental Science Programme (NESP) and the Centre for Southern Hemisphere Oceans Research (CSHOR), a joint research centre between QNLM, CSIRO, UNSW and UTAS. Analysis were conducted on the National Computational Infrastructure (NCI) facility based in Canberra, Australia.

References

Arblaster, J. M., & Meehl, G. A. (2006). Contributions of External Forcings to Southern Annular Mode Trends. *Journal of Climate*, *19*(12), 2896–2905. https://doi.org/10.1175/JCLI3774.1

Baines, P. G., & Fraedrich, K. (1989). Topographic Effects on the Mean Tropospheric Flow Patterns around Antarctica. *Journal of the Atmospheric Sciences*, *46*(22), 3401–3415. https://doi.org/10.1175/1520-0469(1989)046<3401:TEOTMT>2.0.CO;2

Clem, K. R., Renwick, J. A., & McGregor, J. (2017). Large-Scale Forcing of the Amundsen Sea Low and Its Influence on Sea Ice and West Antarctic Temperature. *Journal of Climate*, *30*(20), 8405–8424. https://doi.org/10.1175/JCLI-D-16-0891.1

Dee, D. P., Uppala, S. M., Simmons, A. J., Berrisford, P., Poli, P., Kobayashi, S., et al. (2011). The ERA-Interim reanalysis: configuration and performance of the data assimilation system. *Quarterly Journal of the Royal Meteorological Society*, *137*(656), 553–597. https://doi.org/10.1002/qj.828

England, M. R., Polvani, L. M., Smith, K. L., Landrum, L., & Holland, M. M. (2016). Robust response of the Amundsen Sea Low to stratospheric ozone depletion. *Geophysical Research Letters*, *43*(15), 8207–8213. https://doi.org/10.1002/2016GL070055

Fogt, R. L., Wovrosh, A. J., Langen, R. A., & Simmonds, I. (2012). The characteristic variability and connection to the underlying synoptic activity of the Amundsen-Bellingshausen Seas Low. *Journal of Geophysical Research: Atmospheres*, *117*(D7). https://doi.org/10.1029/2011JD017337

Goyal, R., Sen Gupta, A., Jucker, M., & England, M. H. (2020a). Historical and projected changes in the Southern Hemisphere surface westerlies. *Submitted to Geophysical Research Letters*, (under review).

Goyal, R., Jucker, M., Sen Gupta, A., Hendon, H. H. & England, M. H. (2020b) Zonal Wave 3 Pattern in the Southern Hemisphere generated by tropical convection. *Submitted to Nature Geoscience*, (under review)

Hosking, J. S., Orr, A., Marshall, G. J., Turner, J., & Phillips, T. (2013). The Influence of the Amundsen–Bellingshausen Seas Low on the Climate of West Antarctica and Its Representation in Coupled Climate Model Simulations. *Journal of Climate*, *26*(17), 6633–6648. https://doi.org/10.1175/JCLI-D-12-00813.1

Hosking, J. S., Orr, A., Bracegirdle, T. J., & Turner, J. (2016). Future circulation changes off West Antarctica: Sensitivity of the Amundsen Sea Low to projected anthropogenic forcing. *Geophysical Research Letters*, *43*(1), 367–376. https://doi.org/10.1002/2015GL067143

Inatsu, M., & Hoskins, B. J. (2004). The Zonal Asymmetry of the Southern Hemisphere Winter Storm Track. *Journal of Climate*, *17*(24), 4882–4892. https://doi.org/10.1175/JCLI-3232.1

Lachlan-Cope, T. A., Connolley, W. M., & Turner, J. (2001). The role of the non-axisymmetric antarctic orography in forcing the observed pattern of variability of the Antarctic climate. *Geophysical Research Letters*, *28*(21), 4111–4114. https://doi.org/10.1029/2001GL013465

Neale, R. B., Richter, J. H., Conley, A. J., Park, S., Lauritzen, P. H., Gettelman, A., & Williamson, D. L. (2010). Description of the NCAR Community Atmosphere Model (CAM 4.0). *NCAR Technical Note*, *TN-485*(April), 1–196.

Oleson W Keit, Lawrence M David, Bonan B Gordon, Flanner G Mark, Kluzek Erik, Lawrence J Peter, Levis Samuel, Swenson C Sean, T. E. P. (2010). Technical Description of version 4.0 of the Community Land Model (CLM). *NCAR Technical Note*, *TN-478*(April), 1–238.

https://doi.org/http://dx.doi.org/10.5065/D6FB50WZ

Parish, T. R., & Cassano, J. J. (2003). The Role of Katabatic Winds on the Antarctic Surface Wind Regime. *Monthly Weather Review*, *131*(2), 317–333. https://doi.org/10.1175/1520-0493(2003)131<0317:TROKWO>2.0.CO;2

Peña-Ortiz, C., Manzini, E., & Giorgetta, M. A. (2019). Tropical Deep Convection Impact on Southern Winter Stationary Waves and Its Modulation by the Quasi-Biennial Oscillation. *Journal of Climate*, *32*(21), 7453–7467. https://doi.org/10.1175/JCLI-D-18-0763.1

Pope, J. O., Holland, P. R., Orr, A., Marshall, G. J., & Phillips, T. (2017). The impacts of El Niño on the observed sea ice budget of West Antarctica. *Geophysical Research Letters*, *44*(12), 6200–6208. https://doi.org/10.1002/2017GL073414

Raphael, M. N., Marshall, G. J., Turner, J., Fogt, R. L., Schneider, D., Dixon, D. A., et al. (2016). The Amundsen Sea Low: Variability, Change, and Impact on Antarctic Climate. *Bulletin of the American Meteorological Society*, *97*(1), 111–121. https://doi.org/10.1175/BAMS-D-14-00018.1

Thompson, D. W. J., Solomon, S., Kushner, P. J., England, M. H., Grise, K. M., & Karoly, D. J. (2011). Signatures of the Antarctic ozone hole in Southern Hemisphere surface climate change. *Nature Geoscience*, *4*(11), 741–749. https://doi.org/10.1038/ngeo1296

Trenberth, K. E., Branstator, G. W., Karoly, D., Kumar, A., Lau, N.-C., & Ropelewski, C. (1998). Progress during TOGA in understanding and modeling global teleconnections associated with tropical sea surface temperatures. *Journal of Geophysical Research: Oceans*, *103*(C7), 14291–14324. https://doi.org/10.1029/97JC01444

Turner, J., Phillips, T., Hosking, J. S., Marshall, G. J., & Orr, A. (2013). The Amundsen Sea low. *International Journal of Climatology*, *33*(7), 1818–1829.

https://doi.org/10.1002/joc.3558

Turner, J., Lu, H., White, I., King, J. C., Phillips, T., Hosking, J. S., et al. (2016). Absence of 21st century warming on Antarctic Peninsula consistent with natural variability. *Nature*, *535*(7612), 411–415. https://doi.org/10.1038/nature18645

Walsh, K. J. E., Simmonds, I., & Collier, M. (2000). Sigma-coordinate calculation of topographically forced baroclinicity around Antarctica. *Dynamics of Atmospheres and Oceans*, *33*(1), 1–29. https://doi.org/https://doi.org/10.1016/S0377-0265(00)00054-3

Yiu, Y. Y. S., & Maycock, A. C. (2019). On the Seasonality of the El Niño Teleconnection to the Amundsen Sea Region. *Journal of Climate*, *32*(15), 4829–4845. https://doi.org/10.1175/JCLI-D-18-0813.1

Yiu, Y. Y. S., & Maycock, A. C. (2020). The linearity of the El Niño teleconnection to the Amundsen Sea region. *Quarterly Journal of the Royal Meteorological Society*, *146*(728), 1169–1183. https://doi.org/10.1002/qj.3731

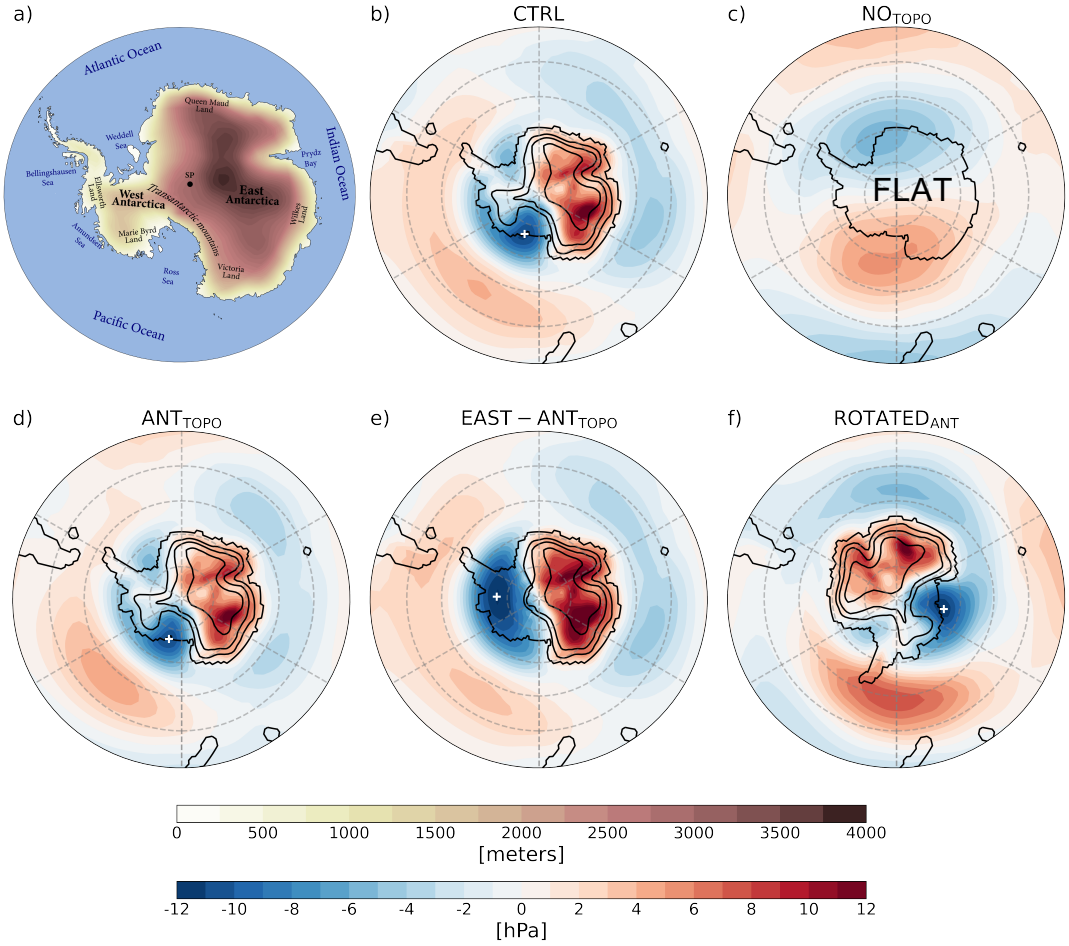

Figure 1 | Model experimental setup and ASL patterns in the different model simulations. Shading in Panel a) shows map of Antarctic topography in metres, with major geographic locations also indicated. Shading in panels (b)-(f) shows the climatological mean sea level pressure from 100 years of model simulations, with the zonal mean removed. The white plus symbol represents the location of the climatological ASL in each experiment. Black contours represent topography of Antarctica in different simulations at every 1000-m interval.

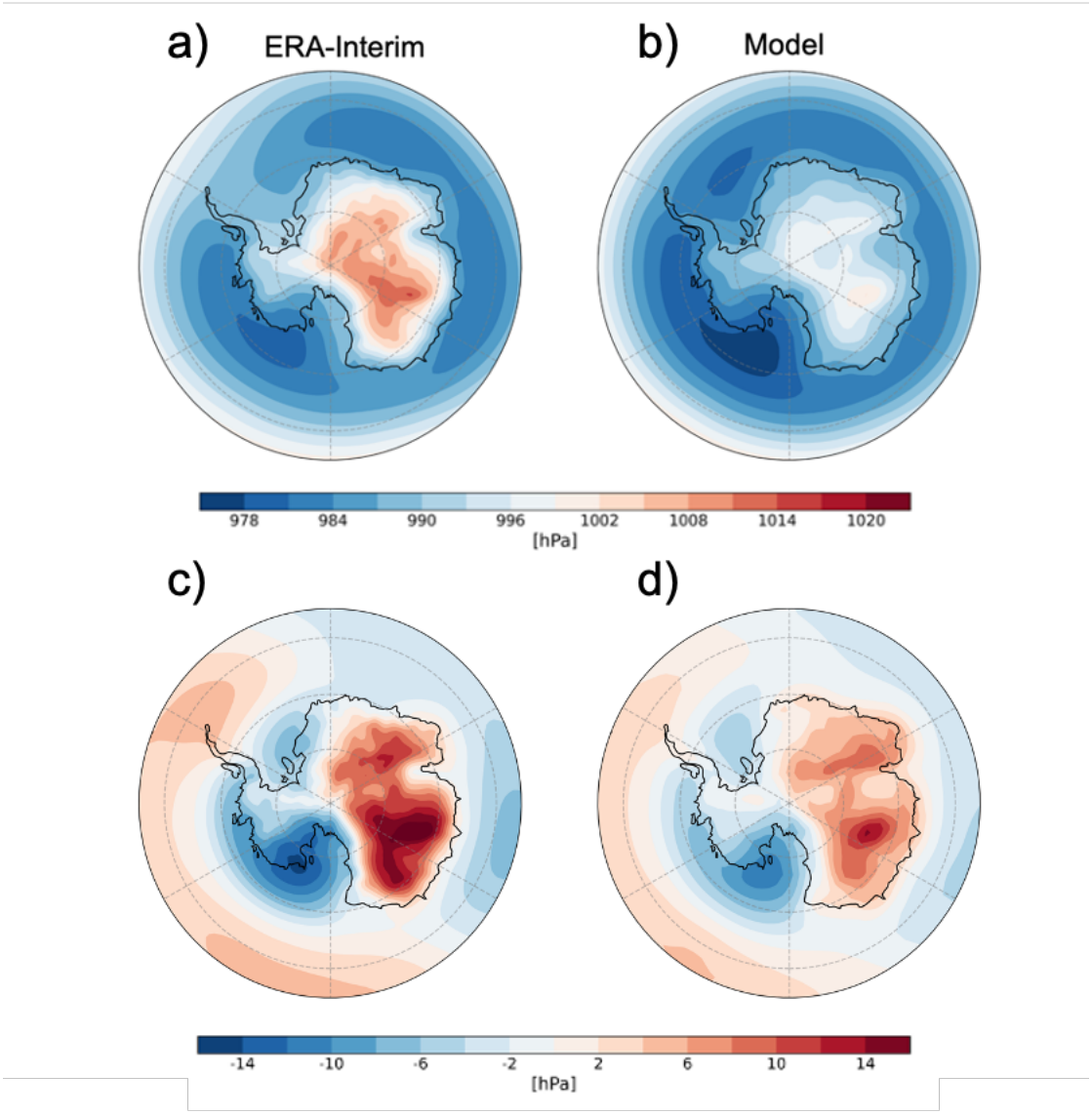

Figure 2 | Comparison of climatological mean ASL in ERA-interim and the *CTRL* simulation. Shading in panels a) and b) show the climatological mean MSLP in ERA-interim and the *CTRL* simulation respectively. Panels c) and d) represent the climatological mean MSLP respectively in ERA-Interim and the *CTRL* simulation when the zonal mean has been subtracted.

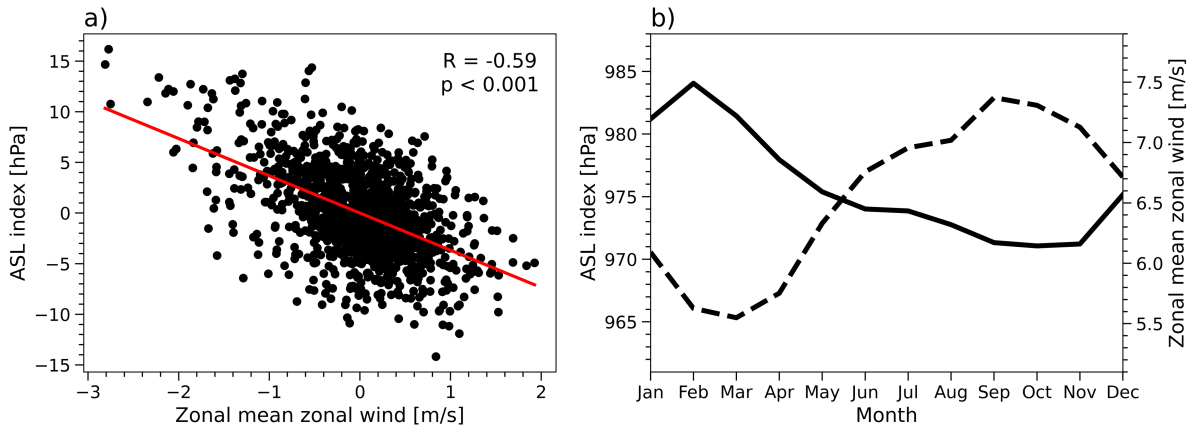

Figure 3 | Relationship between large-scale mid-latitude surface westerlies and the ASL. Panel (a) show scatterplot of the monthly anomalies of the ASL index with the monthly anomalies of the surface (at 60-m elevation) zonal-mean zonal wind averaged between 40-60°S for the *CTRL* simulation. R indicates the correlation coefficient and *p* denotes the p-value of the correlation, while the red line indicates the linear fit line. Dashed and solid black lines in panel (b) represent the monthly climatology of the surface zonal-mean zonal wind averaged between 40-60°S and the monthly climatological ASL index, respectively.

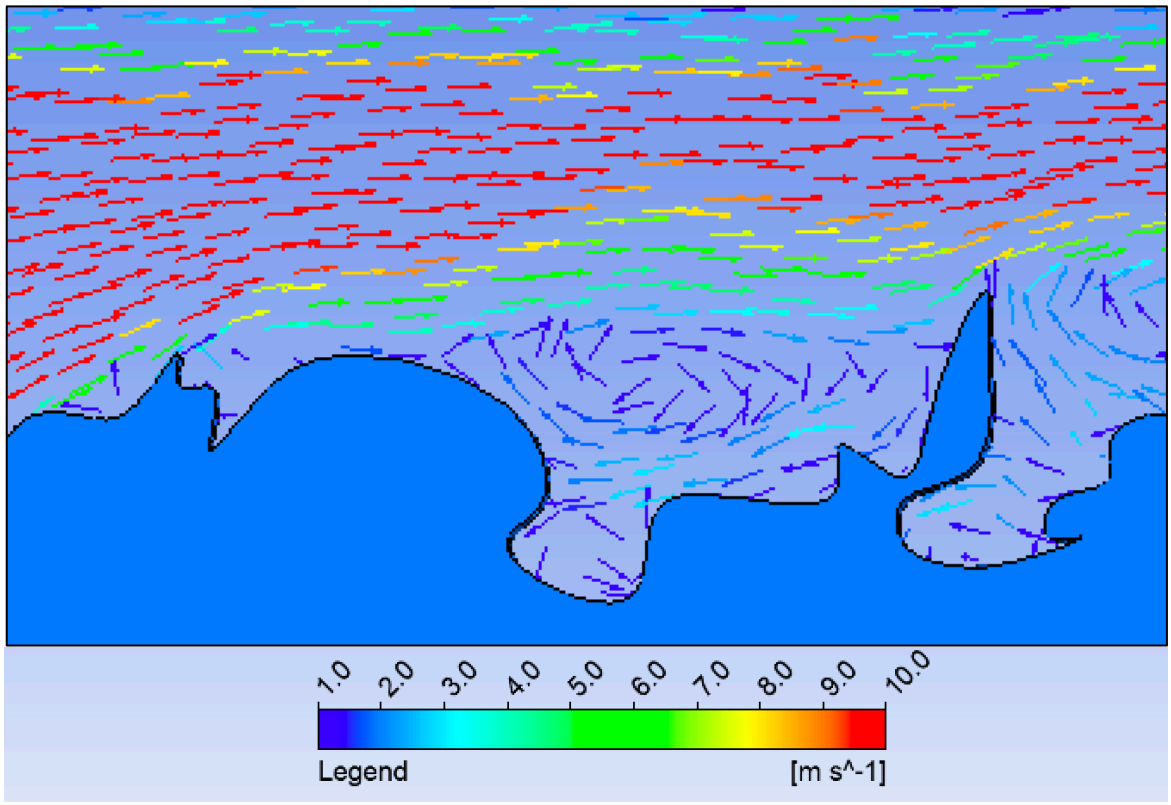

Figure 4 | Non-rotating barotropic flow simulation using a 3D model of Antarctica placed in a 10 m/s westerly wind flow. Vectors represent the direction of the wind and colours represent the magnitude of the wind velocity.